Cooling effect of direct green façades during hot summer days: An observational study in Nanjing, China using TIR and 3DPC data

Haiwei Yin[a,*], Fanhua Kong[b], Ariane Middel[c], Iryna Dronova[d], Hailong Xu[a], Philip James[e]

[a] Department of Urban Planning and Design, Nanjing University, No. 22, Hankou Road, 210093, Nanjing, China

[b] International Institute for Earth System Science (ESSI), Nanjing University, Xianlin Ave. 163, 210023, Nanjing, China

[c] School of Geographical Sciences and Urban Planning, Arizona State University, Tempe, AZ, 85287, United States

[d] Department of Landscape Architecture and Environmental Planning, University of California at Berkeley, Berkeley, CA, 94720, United States

[e] School of Environment and Life Sciences, University of Salford, Salford, M5 4WT, UK

Highlights

• Direct green façades (DGFs) are being applied to buildings in high density cities.

• A new methodology to evaluate DGFs' fine-scale cooling effect is presented.

• DGF enables 4.67 and 8.03 °C maximum surface temperature reduction compared to bare wall at overall and pixel scales.

• DGF cooling effect is most obvious around midday and significantly decreases at night.

• Surface temperatures of DGF exhibit significant spatial variations at pixel scale.

Abstract

Thermal regulation is a key ecosystem service provided by direct green façades (DGFs), as vegetated walls absorb short wave radiation, reduce solar re-radiation from hard surfaces, and provide cooling due to shading and evapotranspiration. Few studies have investigated the correlation between the cooling effect of DGFs and vegetation characteristics at a fine spatial and temporal scale. This paper presents a new methodology to evaluate the cooling effect of DGFs related to fine-scale plant characteristics for hot summer days using thermal infrared (TIR) and three-dimensional point cloud (3DPC) data, through a case study conducted at the Executive Office Building on Nanjing University's Xianlin Campus, China. Results show that daily mean DGF surface temperature is significantly lower than the average bare wall surface temperature, with a maximum reduction of 4.67 °C. The cooling

effect of the DGF is most obvious during midday (10:30 h to 16:00 h) and significantly decreases at night. At the pixel scale, the DGF exhibits a significant spatial variation of surface temperatures, which may be closely related to the DGF's canopy structure. Among the four vegetation indices acquired based on 3DPC data, the percentage of green coverage and the cooling effect of the DGF exhibited a linear relationship, while plant thicknesses, point density, and volume of the green façade were power function distributions. Incoming solar radiation and air temperature are the dominant independent variables in cooling effect and surface temperature fitting models. Our findings can guide DGF design to cool the thermal environment more effectively and to enhance building energy savings.

Keywords

- Cooling effect;
- Direct green façade;
- Plant characteristics;
- Thermal infrared images;
- Three-dimensional point cloud

Introduction

A building's skin has a significant impact on a building's overall energy performance by controlling the absorption of solar radiation and subsequent heat transfer [8]. Greening building walls with vegetation is an effective method to reduce building skin temperature through thermal insulation and to improve the urban thermal environment through shading and evapotranspiration [9,32,36,38]. In general, vertical greening systems (VGSs) can be classified into green façades and living wall systems (LWS) depending on their growing methods [5,27,34,40]. Green façades use climbing plants (lianas, vines, and scramblers) to cover the walls. They offer a flexible and adaptable tool for environmental design [26] and can further be classified into direct and indirect (double-skin) green façades [11,21,27]. Direct green façades (DGFs) are constructed by attaching plants directly to the wall. Indirect or double-skin green façades include a supporting structure for vegetation. As low-cost, easily applicable vertical greening systems [33], DGFs offer additional greening potential for high density urban areas where space for shade trees is limited, but many high-rise building walls exist [5,14]. The potential to use DGFs may be even greater in areas of low- and medium-rise residential, industrial, and commercial buildings in large, sprawled cities [11].

Previous studies have found that green façades, like other types of VGSs, have abundant environmental, economic, and social benefits [11,21,34], including the reduction of greenhouse gas emissions [22] and noise disturbance [13,39]; improving air quality [30]; reducing ambient temperature and, therefore, yielding building energy savings [1,4,8e10,18,25,29,34,38]; creating habitat [19]; and improving aesthetics [37]. However, most studies have focused on the cooling effect of green façades in climates with hot summers, comparing temperatures of vegetated and bare walls using experimental samples, meteorological observing instruments, and mathematical models [11,20,34,36]. For instance, in a study evaluating the thermal effects of different green wall systems [39], measured a reduction of 3.3 °C in ambient air temperature, which corresponded to a 1.1–

11.6 °C decrease in the façade surface temperature immediately behind the vegetation, depending on vegetation type.

In recent years, many studies have evaluated the plant species, their physiological characteristics (e.g. canopy area, canopy density or shadow, leaf area index (LAI), number of leaf layers, plant thicknesses), and relationships with weather parameters (air temperature, relative humidity, solar radiation, wind speed), and wall surface temperature [4,9,12,17,28,31,36,39]. Koyama et al. [17] investigated the relationship between the percent wall coverage of five vine species and reductions in wall surface temperature using freestanding walls. They found percent coverage to be the key variable determining the overall cooling effect. Susorova et al. [36] concluded, from a one-week long observational study, that LAI has a significant influence on façade temperature. They also showed that the most important weather parameters were, in order of decreasing importance: solar radiation, wind speed, relative humidity, and outdoor air temperature. These studies highlight the importance of plant physiology and weather parameters for the overall cooling effect of green façades. However, few scientific investigations have quantified this cooling effect at a high spatial resolution within individual walls, because it is difficult to acquire temperature data and vegetation characteristics at such a fine scale [12,18]. With the development of LiDAR-based sensing techniques, the use of terrestrial laser scanning (TLS) to quantify plant characteristics such as LAI, plants thicknesses, and density has grown rapidly [7,16,23,35,43]. To date, TLS has mainly been used to measure structural tree or forest canopy parameters; little research has been conducted on climbing plant characteristics of green façades [2].

Given the significant influence of plant characteristics on the cooling effect of DGFs and the limited ability of traditional methods to precisely quantify structural vegetation parameters (e.g. percent coverage, plant thicknesses or density), this study was conducted to 1) describe plant characteristics of a DGF using three-dimensional point cloud (3DPC) data acquired through TLS; 2) collect thermal infrared (TIR) data to describe the spatial variation of wall surface temperature at high resolution; 3) identify and evaluate the impact of fine-scale plant characteristics and weather parameters on the cooling effect and the surface temperature of the DGF on hot summer days.

2. Experiment and methods

The study was conducted in Nanjing, the capital of Jiangsu Province, China, divided by the Yangtze River (Fig. 1 a, b). Nanjing covers an area of 4723 km^2, and had a population of approximately 6.5 million in 2014 [24]. Nanjing has a subtropical monsoon climate with four seasons including a hot and humid summer. The mean annual temperature is 15 °C, with a mean daily maximum temperature of 31 °C between June and August. Between 1951 and 2016, Nanjing experienced 127 summer heat wave events, defined as three consecutive days when the daily maximum temperature equals to or exceeds 35 °C [16,41]. Per capita public green space in Nanjing has increased rapidly since the implementation of Urban Green Space System (UGSS) planning in 1997, from 8m^2 to 15m^2 in 2014. However, most green spaces are not vertical systems; only few DGFs have been constructed on public buildings, including schools, universities, and hospitals.

Field observations were carried out during three hot summer days on the façade of the Executive Office Building at Nanjing University Xianlin Campus (Fig. 1c, d, e). The building faces south and is a three story brick-concrete composite structure (Fig. 2a). The façade facing south is covered with climbing ivy (*Parthenocissus tricuspidata*), planted in 2011. In this study, we chose the western part of the south-facing building wall as experimental surface (Fig. 2a,b).

2.2. Data acquisition

Microclimate measurements were conducted at the study site during the only summer heat wave event in 2015 (July 28 to August 6) from August 4 to 6. A meteorological station (HOBO U30) was set up 1 m away from the building wall (Fig. 2a) to record air temperature (Ta), solar radiation (SR), relative humidity (RH), wind speed (WS), and wind direction (WD) in front of the DGF (Table 1). Light intensity at the wall behind the plant canopy was measured using a solar radiation sensor (BSR, shown in Fig. 2a). All data were recorded at 1-min intervals and stored in a data logger. TIR data were acquired between August 4, 15:45 h, and August 6, 18:00 h at 15-min intervals using an infrared imaging device (Testo890) with a predefined sampling resolution of 640 x 480 pixels (Fig. 2b). A Riegl VZ-400 TLS device was set up in front of the building to acquire raw 3DPC data in a high-speed mode with a sampling resolution of 3 mm at 100 m distance from the scanner and a beam divergence of 0.35 mrad (Fig. 2c and d).

2.3. Data processing

The cooling effect of the DGF at any given time and for any pixel, i.e. the surface temperature reduction (DTi), was defined as the difference between the surface temperature at each ivy covered building façade pixel (Ts_Gi) and the mean surface temperature of all non-vegetated (bare) building façade pixels (Ts_B_mean). Based on the TIR and 3DPC data, the surface temperature of each building façade pixel as well as four plant characteristics, i.e. percentage of green coverage (PGC), plant thicknesses (PT), 3DPC point density of the green façade (PD_{3DPC}), and 3DPC volume of the green façade (VG_{3DPC}), were determined as described below.

2.3.1. Surface temperature and cooling effect (ΔTi)

All TIR data were pre-processed manually in TestoIRSoft (Version 3.6, Testo SE&Co. KGaA), using an emissivity value of 0.95 and meteorological data observed at the HOBO automated station. We performed a grid transform and geometric correction of the pre-processed TIR data in ArcGIS, using 3DPC data as spatial reference at a pixel size of 0.1 m x 0.1 m. Then, we obtained the façade surface temperature Ti for each pixel, windows excluded (Fig. 3a). Finally, the 3DPC point cloud of the DGF was used to classify each pixel as vegetated (one or more 3DPC points) or non-vegetated (no 3DPC points). The surface temperature reduction ΔTi was calculated for all vegetated pixels (Fig. 3b).

2.3.2. Plant characteristics

To obtain plant characteristics from TLS data, the 3DPC was pre-processed using Cyclone and MATLAB (Version 7.10, Mathworks Inc.). The resultant point cloud was imported in ArcGIS with x and y coordinates serving as the spatial reference. The z value, denoting the distance of each point from the façade, was stored in the attribute table. Because of the boundary effects, points near windows were deleted using a 0.1 m buffer distance (Fig. 4a).

Finally, vegetated points of the DGF were obtained by deleting points with a distance from the wall of z ≤0.01 m (Fig. 4b). The four plant characteristics were calculated as outlined below.

(1) Percentage of Green Coverage (PGC)

PGC is a two-dimensional parameter that denotes the degree of vegetation cover of a façade [11]. Previous research strongly suggests that PGC significantly impacts the magnitude of cooling a green façade provides [12,17]. Traditionally, PGC has been calculated from binary images of green façades that were derived from digital photos using image processing. In this study, PGC at pixel scale (0.1 m x 0.1 m) is calculated as the ratio of vegetated façade area (including leaves, branches, and stem) to wall area, obtained from the 3DPC of the DGF (Figs. 4b and 5a). First, a 5 mm buffer of green façade point data was created in ArcGIS. Then, the buffer polygons were cut by the vector fishnet file (0.1 m x 0.1 m) of the study area, and the area covered by plants at the pixel scale (SGi) was calculated using Spatial Join tool in ArcGIS. The percentage of green coverage at each pixel (PGCi) was obtained using Eq. (1) (Fig. 5a).

$$PGC_i = \frac{SG_i}{S_i} \times 100\% \quad (1)$$

In the above equation, SGi is the total area covered by plants in cell i; PGCi is the percentage of green coverage of pixel i; Si is the area of cell i, = 0.1 x 0.1 m, i.e., 0.01 m^2.

Plant thicknesses (PT) Similar to LAI or number of leaf layers, plant thickness (PT) is a measure of the climbing plant canopy density [11]. Most studies highlight the strong inverse relationship between the cooling effect of green façades and plant thickness, LAI, or number of leaf layers, because climbing plants significantly reduce a wall's solar access [6,12,36,39]. In this study, the plant thickness PTi in a pixel, i.e., the mean thicknesses of the green façade at pixel scale, represented the mean distance of all DGF points from the wall, as derived from 3DPC data in ArcGIS (Fig. 5b).

(2) Point density of 3DPC of green façade (PD_{3DPC})

Three-dimensional greening quantity (i.e., the spatial volume formed by the stem and leaves of a plant) is an important parameter to evaluate the ecosystem service benefits of green infrastructure [16]. Given the limited ability of traditional methods to precisely quantify this parameter, few studies have investigated the relationship between vegetation mass and cooling effect of green façades at a fine scale [12], although previous studies have identified a strong influence of vegetation mass on cooling performance for tree canopies [16,23]. In this study, the three-dimensional greening quantity PD3DPC of the DGF was approximated as the number of points in the 3DPC of the green façade in each pixel (Fig. 5c).

(4) Volume of 3DPC of green façade (VG_{3DPC})

The parameter VG3DPC was defined as the volume of the convex hull created by the 3DPC of the green façade in a given bounding box of 0.1 m x 0.1 m x 0.25 m. VG_{3DPC} approximates the three-dimensional spatial extent of the climbing ivy. As 3D parameter, it is a better approximation of the three-dimensional greening quantity than the parameter PD_{3DPC}. The bounding box and convex hull were constructed in MATLAB and VG3DPC for each given

bounding box was calculated in ArcGIS (Fig. 5d). More details about these methods can be found in Ref. [43].

2.4. Statistical analysis

Next, we performed a statistical analysis of variability in cooling effect indicators and their associations with key meteorological variables and vegetation characteristics. First, we selected four façade snapshots at different times for August 4 and August 6 and quantified the maximum, minimum, mean and standard deviation of DTi. Next, we conducted a multiple linear regression analysis to determine which weather parameters were most strongly associated with the mean surface temperature of the bare wall (Ts_B_mean), the mean surface temperature of the DGF (Ts_G_mean), and the cooling effect (the difference between Ts_G_mean and Ts_B_mean). This analysis was performed using a stepwise selection method, and standardized model coefficients, the coefficient of determination (R2) and model p-value were used as criteria to identify the strongest predictors. Finally, we estimated Pearson's correlation coefficients and univariate regression relationships between the four plant indices (PGC, PT, PD_{3DPC} and VG_{3DPC}) and the cooling effect ΔT at different times of day (two tailed test) to determine the relative importance of these different vegetation properties in the cooling performance of the DGF.

3. Results

3.1. Variability of DGF cooling at the façade scale

Overall, the DGF exhibited a significant cooling effect during our study period from August 4 to August 6, 2015. Based on 43 sampled records, the mean vegetated surface temperature was significantly lower than the surface temperature of the bare façade (Fig. 6). The maximum and minimum surface temperature reduction were 4.67 °C (12:30 h, Aug. 6, 2015) and 0.74 °C (19:45 h, Aug.4, 2015), respectively; the mean surface temperature reduction was 2.56 °C. During middle of day (10:30 h - 16:00 h), the mean surface temperature reduction was almost at its peak with 4.07 °C. In this period, mean SR and BSR were approximately 800W/m2 and 50 W/ m2, respectively, and leaf transmissivity (BSR/SR) was lower than 20% (Fig. 7). The cooling effect started to decrease at 16:00 h when SR was generally below 50 W/m2 (Fig. 7). The cooling effect was minimal after sunset (19:00 h), with a mean surface temperature reduction of only 0.83 °C. During the day (05:22 h - 19:00 h), the BSRwas significantly lower than the SR (47 W/m^2 and 434 W/m^2 on average), i.e., the DGF reduced about 89.17% of the solar radiation. These findings suggest that the cooling effect of DGFs on hot summer days is mainly due to shading on the building façade (Fig. 7).

3.2. Variability of DGF cooling at pixel scale

For a fine-scale visual analysis of ΔTi, we selected four façade snapshots at different times for August 4 (Fig. 8) and August 6 (Fig. 9); results of the statistical analysis of all sampling data are shown in Fig. 10. Figs. 8 and 9 illustrate a significant spatial variability in DGF cooling at the pixel scale, which may be closely related to the canopy structure of the DGF (Fig. 5). The cooling impact of the DGF at the pixel scale was rapidly diminished as incoming solar radiation dropped in the late afternoon of August 4 (Figs. 7 and 8). At 16:45 h, the cooling effect of most vegetated pixels ranged between 2.50 and 2.99 °C, but at 17:45 h, 18:45 h and 20:45 h, it decreased to 1.50–1.99 °C, 1.00–1.49 °C, and 0.50–0.99 °C, respectively (Fig. 8). On August 6, the cooling effect of the DGF was highly significant during midday with maximum ΔTi 8.03 °C; most vegetated pixels were more than 4.5 °C cooler (Fig.

9). Even at 17:00 h, maximum ΔTi was larger than 4.5 °C and most of the pixels were more than 3.5 °C cooler, which indicates a significantly higher temperature reduction than on August 4 for the same time of day (Fig. 10a). This is mainly because the solar radiation observed between 16:00 h and 18:00 h was significantly higher on August 6 than on August 4 (Fig. 7).

A regression analysis of all sampling records showed that the maximum pixel-scale temperature reduction of the DGF and its standard deviation were linearly correlated (R^2 = 0.89), i.e., the larger ΔTi, the greater was the variability of ΔTi (Fig. 10). For example, ΔTi peaked at 6.5 °C at 16:00 h on August 6, with a high standard deviation of 3.1 °C (Fig. 10a), indicating large spatial variability of the DGF's cooling effect at the pixel scale. However, around midday (10:30 h – 13:45 h) this relationship did not hold (see colored regions in Fig. 10a and b): ΔTi was large (6–8 °C), but the standard deviations was less than 1.5 °C. At about 10:30 on this hot summer day, the solar radiation was over 800 W/m2 and the air temperature exceeded 35 °C (Fig. 7). High temperature and radiation suppressed the evapotranspiration potential of the DGF, making shading the dominant cooling factor for the DGF [9]. This result indicates that the canopy structure of the DGF (e.g., PGC) is the dominant factor influencing the spatial variability of the cooling effect during hot sunny summer days.

3.3. Relationship between the overall DGF cooling effect and weather parameters

Multiple linear regression analysis showed that the mean surface temperature of the bare wall (Ts_B_mean), the mean surface temperature of the DGF (Ts_G_mean), and the cooling effect (the difference between Ts_G_mean and Ts_B_mean) can be explained through weather characteristics (Table 2). The adjusted R2 of the model was larger than 0.7, and the t-tests and levels of significance for the regression coefficients show that all regression coefficients were significantly different (sig. < 0.05). The air temperature (Ta) was the dominant independent variable of the fitting models explaining Ts_B_mean and Ts_G_mean with standardized coefficients greater than 1.1. Relative humidity (RH) was the second major factor; standardized coefficients were 0.639 and 0.392, respectively. Wind speed (WS) also had an impact on the surface temperature (standardized coefficients values are 0.324 and 0.225, respectively), while solar radiation (SR) was excluded, because it failed to pass the F test in the analysis process. This may be due to the high correlation between solar radiation (SR) and air temperature (T_a) (the correlation coefficient was 0.485 and significant at 0.01 level), and the changes of SR impacts the T_a some time later, as suggested by Fig. 7. However, solar radiation (SR) was the strongest statistical predictor in the model for the cooling effect, the standardized coefficients value was -0.553 (Table 2). Relative humidity (RH) and wind speed (WS) had a similar influence, their standardized coefficients values were -0.324 and -0.293, respectively. Collectively, these results indicate that the cooling effect of a green façade on hot summer days occurred mainly due to the shading effect of the greenery canopy.

3.4. Correlation between the cooling effect and plant characteristics at pixel scale

We quantified Pearson's correlation coefficients among the four plant indices and the cooling effect ΔT at different times of day (two-tailed test). Results show that PGC had the highest correlation coefficient of the four vegetation indices (Fig.11). This indicates that

PGC is an important factor in determining the cooling benefits of DGFs, and that shading on the building façade through vegetation is highly correlated with the cooling of DGFs. The correlation coefficients exhibited a similar temporal trend across the four indices, but PT performed less well during certain times of day and, therefore, could not characterize the shading effect of the DGF as accurately as the other three indices (Fig. 11).

To explore the relationship between the four plant indices and the mean surface temperature of all vegetated building façade pixels (Ts_G_mean), univariate regression analysis was applied to field observations from 13:45 h on August 6, 2015 and 20:45 h on August 4, 2015 as examples. Although the change curves have the same trend, there was a smoother relationship between the Ts_G_mean and the four vegetation indices at 20:45 on August 4,2015 than at 13:45 on August 6, 2015 (Figs. 12 and 13). Meanwhile the relationship between PGC and Ts_G_mean was linear with a negative trend, the relationship between the other three indices and Ts_G_meanwas exponential (Figs.12 and 13). This suggests that the PGC is an index that can better characterize the cooling effect of DGFs (Figs. 12a and 13a) than the other three indices. For example, PT characterizes the mean canopy thickness of the DGF at the pixel level. The scatter plot between PT and Ts_G_mean yielded a twostage distribution, and 0.04 m was the demarcation point between the two phases (Figs. 12b and 13b). With PT smaller than 4 cm, the cooling effect decreased greatly with a slight increase in PT; with PT larger than 4 cm, the cooling effect was reduced slowly when PT increased greatly. This shows that the DGF can produce an obvious cooling effect as long as there is thin vegetation cover, and the variation of the cooling effect becomes very small with increasing PT (Figs. 12b and 13b). The curves of the PD3DPC and VG3DPC indices versus Ts_G_mean (Fig. 12 c, d, Fig. 13 c, d) were similarly shaped. There are also obvious cutoff points, approximately 60 points of 3DPC and 100 cm3 respectively, but the degree of variations is smaller than that of PT.

4. Discussion

Historically, DGFs have often been used on traditional brick building façades in China and were found to have important ecological effects and aesthetic value. At present, some buildings with six or fewer stories have DGFs, and the majority of those are public buildings. However, with continued urban sprawl, the urban heat island effect is growing and the thermal comfort level in cities is decreasing [3,15,42]. Due to a lack of non built-up land in high density areas, it is difficult to increase the amount of urban green space to alleviate these effects. In recent years, VGSs have received more attention by scholars and urban managers; however, an accurate characterization of the cooling impact of green façades at fine scales is still challenging [2]. In this paper, the cooling effect of a DGF at pixel scale (0.1 m x 0.1 m) and its relationship with vegetation characteristics were quantified based on TIR and 3DPC data through an observational case study. The results provide evidence of a significant surface temperature reduction attributable to DGFs and thus offer valuable information for city managers and decision makers on planning and construction of DGFs.

The four vegetation indices PGC, PT, PD_{3DPC}, and VG_{3DPC} calculated from 3DPC data accurately represented the important characteristics of the DGF, such as vegetation coverage, thickness, density, and three-dimensional vegetation mass. At the pixel scale, percent vegetation cover, thickness, density, and volume of the DGF have a significant impact on cooling performance. While PGC varies linearly with the cooling effect, the other

plant characteristics show an exponential distribution, indicating that vegetation coverage is a better factor affecting façade surface temperatures than the other indices. A good cooling effect can be achieved as long as the vegetation covering the façade has a certain thickness (0.04 m), density (60 points of 3DPC), and green biomass (100 cm^3). The change curves between the Ts_G_mean and the four vegetation indices at 20:45 h on August 4 were smoother than those at 13:45 h on August 6, 2015, and the according R^2 values were smaller (Figs. 12 and 13). This indicates that the plant canopy's impact on the cooling effect of the DGF at night was weaker than that at daytime due to the reduction of evapotranspiration and the absence of sun and shade. Solar radiation (SR) was found to be the most important independent variable explaining façade cooling of the DGF. This provides further evidence that the cooling effect of DGFs in the middle of the day during hot summer days is mainly due to shading on the building façade. Thus, in the process of designing a green façade, it is paramount to improve vegetation coverage on sun-exposed building façades.

Although we conducted an exploratory analysis of the cooling effect of DGF with regard to vegetation characteristics and weather features at the pixel scale in this study, some aspects of this study could be still improved in the future. For example, the TIR observations during the study period were incomplete and only 43 records were sampled to analyze the average cooling effect; also, only 8 samples were collected after sunset (19:00 h – 20:45 h, August 4, 2015). With more complete observational data it will be possible to better characterize nocturnal and seasonal cooling of the DGF. In addition, the relationship between the cooling effect of DGFs and vegetation coverage characteristics may be affected by spatial scale, which needs more research in the future. Thirdly, the laser beam of the TLS cannot penetrate lamina to characterize the vertical canopy structure of the DGF. Therefore, vegetation indices based on 3DPC data can only partially estimate vegetation characteristics of the DGF. More refined techniques and methods to obtain 3DPC data of DGFs need to be explored in the future studies. Fourthly, reflectivity was not measured in this study; instead, a recommended value was used based on the literature. The effects of light-colored versus dark-colored vegetation on the energy balance of the DGF which may potentially produce different cooling effects due to their albedos need further testing in the future. Finally, with the incident angle of the sun varying at different times of the day, the shadow of the vegetation canopy may also influence the cooling effect of many pixels in the marginal zones of non-continuous vegetation canopy [6]. Assessing such marginal impact also requires in-depth analysis in the future studies.

5. Conclusion

Results of this study show that TIR and 3DPC observations can provide valuable information to assess the cooling effect of DGFs at a fine scale. A DGF was found to significantly cool façade surfaces with the maximum average surface temperature reduction of 4.67 °C. The most pronounced cooling effect was observed during the middle of the day (11:00 h – 16:00 h), and it was significantly reduced at night. At the pixel scale, the cooling effect of the DGF exhibited high spatial variability due to differences in the DGF's greenery canopy structure. Around midday (around 10:30 h – 13:45 h), the variability in surface temperature reduction was relatively small (<1.5 °C), because shading on the building façade becomes the dominant factor in façade cooling of the DGF. Among the four vegetation indices derived using 3DPC data, PGC had a strong linear correlation with the cooling effect and thus represents an important green DGF canopy structural factor for cooling of the DGF on hot

summer days. Solar radiation (SR) and air temperature (Ta) appeared to be the dominant independent variables of the cooling effect and surface temperature fitting model, respectively. These findings can be used as a guide for DGF planning and design to improve the outdoor thermal environment and achieve building energy savings.

Acknowledgement
The research was supported by the National Natural Science Foundation of China (No.51478217, 31170444) and Central university basic research and operating expenses of special funding. The authors thank Wenfeng Zhan, Guang Zheng and Lixia Ma for helping data processing; and thank Fengfeng LIU, Xiaojuan Wang and all other members who helped to conduct the field surveys.

References
[1] E. Alexandri, P. Jones, Temperature decreases in an urban canyon due to greenwalls and green roofs in diverse climates, Build. Environ. 43 (2008) 480–493.
[2] H. Attya, A. Habib, D. Al-Obaybi, Developing a three-dimensional geometric framework for greening buildings' façade, Procedia Eng. 118 (2015) 465–469.
[3] A. Buyantuyev, J.G. Wu, Urban heat islands and landscape heterogeneity: linking spatio-temporal variations in surface temperatures to land-cover and socioeconomic patterns, Landsc. Ecol. 25 (2010) 17–33.
[4] R.W.F. Cameron, J.E. Taylor, M.R. Emmett, What's 'cool' in the world of green façades? How plant choice influences the cooling properties of green walls, Build. Environ. 73 (2014) 198–207.
[5] C.Y. Cheng, K.K.S. Cheung, L.M. Chu, Thermal performance of a vegetated cladding system on façade walls, Build. Environ. 45 (2010) 1779–1787.
[6] E. Cuce, Thermal regulation impact of green walls: an experimental and numerical investigation, Appl. Energy (2016). http://dx.doi.org/10.1016/j.apenergy.2016.09.079.
[7] M. Dassot, T. Constant, M. Fournier, The use of terrestrial LiDAR technology in forest science: application fields, benefits and challenges, Ann. For. Sci. 68 (2011) 959–974.
[8] M. Haggag, A. Hassan, S. Elmasry, Experimental study on reduced heat gain through green façades in a high heat load climate, Energy Build. 82 (2014) 668–674.
[9] M.T. Hoelscher, T. Nehls, B. Jänicke, G. Wessolek, Quantifying cooling effects of façade greening: shading, transpiration and insulation, Energy Build. 114 (2016) 283–290.
[10] A. Hoyano, Climatological uses of plants for solar control and the effects on the thermal environment of a building, Energy Build. 11 (1988) 181–199.
[11] A.M. Hunter, N.S.G. Williams, J.P. Rayner, L. Aye, D. Hes, S.J. Livesley, Quantifying the thermal performance of green façades: a critical review, Ecol. Eng. 63 (2014) 102–113.
[12] K. Ip, M. Lam, A. Miller, Shading performance of a vertical deciduous climbing plant canopy, Build. Environ. 45 (2010) 81–88.
[13] M.R. Ismail, Quiet environment, Acoustics of vertical green wall systems of the Islamic urban form, Front. Archit. Res. 2 (2013) 162–177.
[14] C. Jim, H. He, Estimating heat flux transmission of vertical greenery ecosystem, Ecol. Eng. 37 (2011) 1112–1122.
[15] F.H. Kong, H.W. Yin, P. James, L.R. Hutyra, H.S. He, Effects of spatial pattern of greenspace on urban cooling in a large metropolitan area of Eastern China, Landsc. Urban Plan. 128 (2014) 35–47.

[16] F.H. Kong, W.J. Yan, G. Zheng, H.W. Yin, G. Cavan, W.F. Zhan, N. Zhang, L. Cheng, Retrieval of three-dimensional tree canopy and shade using terrestrial laser scanning (TLS) data to analyze the cooling effect of vegetation, Agric. For. Meteorol. 217 (2016) 22–34.
[17] T. Koyama, M. Yoshinaga, H. Hayashi, K-i Maeda, A. Yamauchi, Identification of key plant traits contributing to the cooling effects of green façades using freestanding walls, Build. Environ. 66 (2013) 96–103.
[18] T.C. Liang, W.N. Hien, S.K. Jusuf, Effects of vertical greenery on mean radiant temperature in the tropical urban environment, Landsc. Urban Plan. 127 (2014) 52–64.
[19] F. Madre, P. Clergeau, N. Machon, A. Vergnes, Building biodiversity: vegetated façades as habitats for spider and beetle assemblages, Glob. Ecol. Conservation 3 (2015) 222–233.
[20] L. Malys, M. Musy, C. Inard, A hydrothermal model to assess the impact of green walls on urban microclimate and building energy consumption, Build. Environ. 73 (2014) 187–197.
[21] M. Manso, J. Castro-Gomes, Green wall systems: a review of their characteristics, Renew. Sustain. Energy Rev. 41 (2015) 863–871.
[22] M. Marchi, R.M. Pulselli, N. Marchettini, F.M. Pulselli, S. Bastianoni, Carbon dioxide sequestration model of a vertical greenery system, Ecol. Model. 306 (2015) 46–56.
[23] I. Moorthy, J.R. Miller, J.A.J. Berni, P. Zarco-Tejada, B. Hu, J. Chen, Field characterization of olive (Oleaeuropaea L.) tree crown architecture using terrestrial laser scanning data, Agric. For. Meteorol. 151 (2011) 204–214.
[24] Nanjing Municipal Statistics Bureau, Nanjing Statistical Yearbook, China Statistics Press, Beijing, China, 2014 (in Chinese).
[25] B.A. Norton, A.M. Coutts, S.J. Livesley, R.J. Harris, A.M. Hunter, A.S.G. Williams, Planning for cooler cities: a framework to prioritise green infrastructure to mitigate high temperatures in urban landscapes, Landsc. Urban Plan. 134 (2015) 127–138.
[26] T.R. Oke, The urban energy balance, Prog. Phys. Geogr. 12 (1988) 471–508.
[27] M. Ottelé, K. Perini, A.L.A. Fraaij, E.M. Haas, R. Raiteri, Comparative life cycle analysis for green façades and living wall systems, Energy Build. 43 (2011) 3419–3429.
[28] B.L. Ong, Green plot ratio, an ecological measure for architecture and urban planning, Landsc. Urban Plan. 63 (2003) 197–211.
[29] L. Pan, L.M. Chu, Energy saving potential and life cycle environmental impacts of a vertical greenery system in Hong Kong: a case study, Build. Environ. 96 (2016) 293–300.
[30] A.K. Pandey, Pandey, B.D. Tripathi, Air Pollution Tolerance Index of climber plant species to develop Vertical Greenery Systems in a polluted tropical city, Landsc. Urban Plan. 144 (2015) 119–127.
[31] G. Pérez, L. Rincón, A. Vila, J.M. Gonzalez, L.F. Cabeza, Behaviour of green façades in Mediterranean Continental climate, Energy Convers. Manag. 52 (2011) 1861–1867.
[32] K. Perini, M. Ottelé, E. Haas, R. Raiteri, Greening the building envelope, façade greening and living wall systems, Open J. Ecol. 1 (2011) 1–8, http://dx.doi.org/10.4236/oje.2011.11001.
[33] K. Perini, P. Rosasco, Cost-benefit analysis for green façades and living wall systems, Build. Environ. 70 (2013) 110–121.
[34] T. Safikhani, A.M. Abdullah, D.R. Ossen, M. Baharvand, A review of energy characteristic of vertical greenery systems, Renew. Sustain. Energy Rev. 40 (2014) 450–462.
[35] R. Sanz, J.,R. Rosell, J. Llorens, E. Gil, S. Planas, Relationship between tree row LIDAR-volume and leaf area density for fruit orchards and vineyards obtained with a LIDAR 3D dynamic measurement system, Agric. For. Meteorol. 171 (2013) 153–162.

[36] I. Susorova, M. Angulo, P. Bahrami, B. Stephens, A model of vegetated exterior façades for evaluation of wall thermal performance, Build. Environ. 67 (2013)1–13.
[37] E.V. White, B. Gatersleben, Greenery on residential buildings: does it affect preferences and perceptions of beauty? J. Environ. Psychol. 31 (2011) 89–98.
[38] I. Wong, A.N. Baldwin, Investigating the potential of applying vertical green walls to high-rise residential buildings for energy-saving in sub-tropical region, Build. Environ. 97 (2016) 34–39.
[39] N.H. Wong, A.Y.K. Tan, P.Y. Tan, K. Chiang, N.C. Wong, Acoustics evaluation of vertical greenery systems for building walls, Build. Environ. 45 (2010) 411–420.
[40] N.H. Wong, A.Y.K. Tan, P.Y. Tan, N.C. Wong, Energy simulation of vertical greenery systems, Energy Build. 41 (2009) 1401–1408.
[41] X.Z. Xu, Y.F. Zheng, J.F. Yin, R.J. Wu, Characteristics of high temperature and heat wave in Nanjing City and their impacts on human health, Chin. J. Ecol. 30 (2011) 2815–2820 (in Chinese, with English abstract).
[42] X.S. Yang, L.H. Zhao, M. Bruse, Q.L. Meng, Evaluation of a microclimate model for predicting the thermal behavior of different ground surfaces, Build. Environ. 60 (2013) 93–104.
[43] G. Zheng, L.M. Moskal, Computational-geometry-based retrieval of effective leaf area index using terrestrial laser scanning, IEEE Trans. Geoscience Remote Sens. 50 (2012) 3958–3969.

Table 1
Main sensor parameters of HOBO automated meteorological observing stations.

Smart sensors	Product model	Supported measurement	Accuracy	Resolution	Installation height
Wind speed and direction smart sensor	S-WCA-M003	Wind speed Wind direction	±0.5 m/s ±5	0.19 m/s (0.42mph) 1.4°	1.5 m
Temperature/RH smart sensor	S-THB-M002	Temperature Relative humidity	±0.2 °C (25 °C) ±2.5%	0.02 °C (25 °C) 0.03%	Ta, RH:1.5 m
Solar radiation sensor	S-LIB-M003	Light intensity	±10 W/m2	1.25 W/m2	SR:1.5 m; BSR:2 m

Table 2 Results of the multi-parametric linear stepwise regression.

Model		Unstandardized coefficients		Standardized coefficients	t	Sig.
		B	Std. error	Beta		
Dependent Variable: Ts_B_mean Adjusted R2 - 0.889	(Constant)	-50.829	7.563	—	-6.721	0.000
	Ta	2.004	0.154	1.212	13.057	0.000
	WS	4.543	0.764	0.324	5.948	0.000
	RH	0.339	0.047	0.639	7.156	0.000
Dependent Variable: Ts_G_mean Adjusted R^2 = 0.928	(Constant)	-29.357	5.102	—	-5.754	0.000
	Ta	1.600	0.104	1.153	15.452	0.000
	WS	2.643	0.515	0.225	5.130	0.000
	RH	0.174	0.032	0.392	5.456	0.000
Dependent Variable: ΔT Adjusted R^2 = 0.701	(Constant)	1.495	0.964	—	1.551	0.029
	SR	-0.002	0.000	-0.553	-4.903	0.000
	RH	-0.053	0.016	-0.324	-3.273	0.002
	WS	-1.260	0.494	-0.293	-2.551	0.015

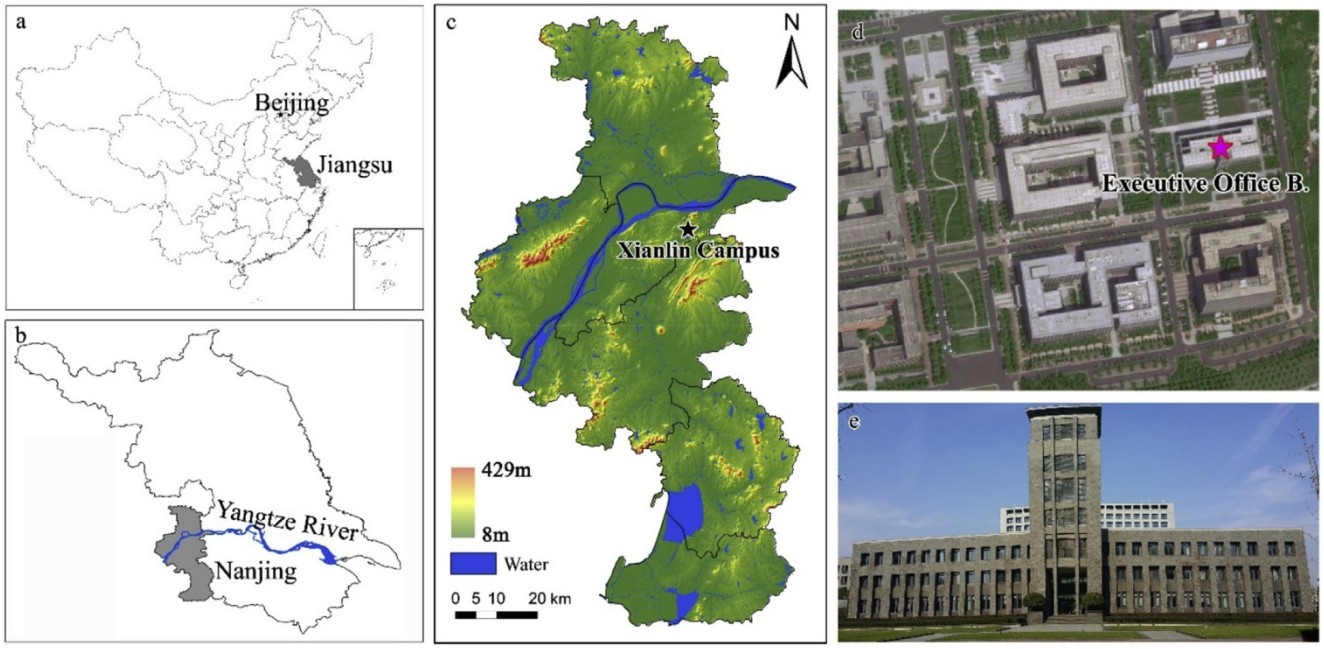

Fig. 1. Study area and observation sites.

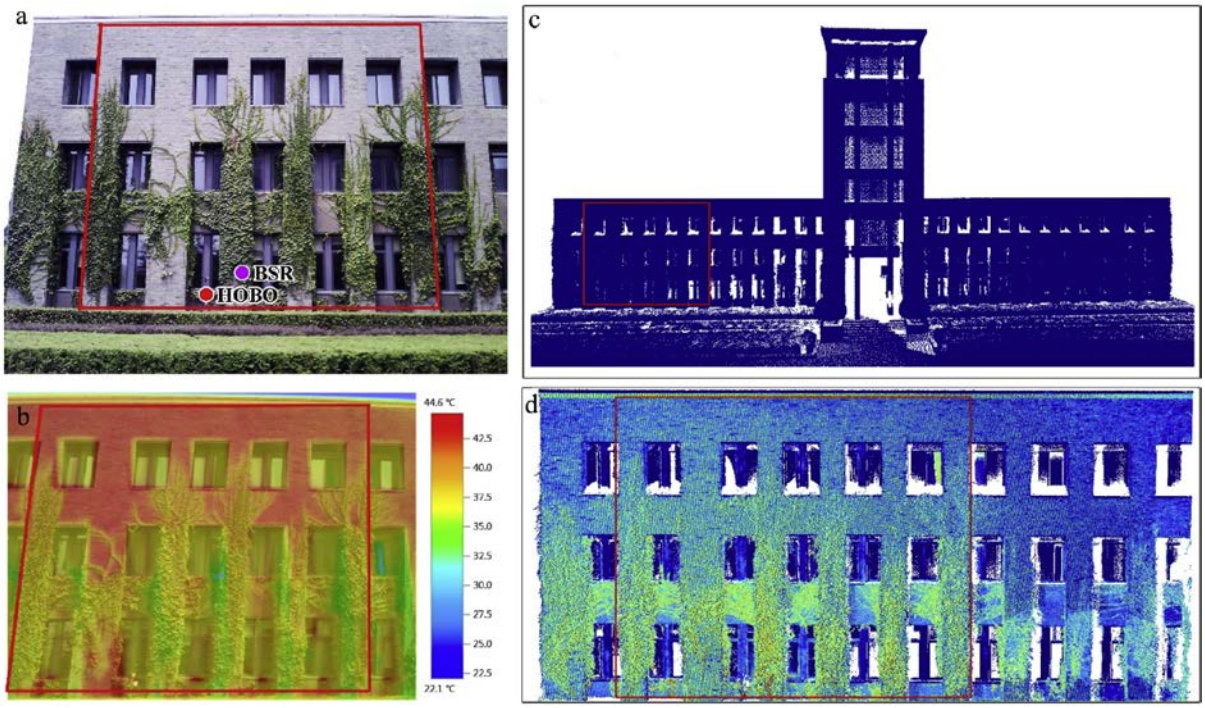

Fig. 2. Experimental building façade area (a) and raw TIR (b) and 3DPC (c, d) data.

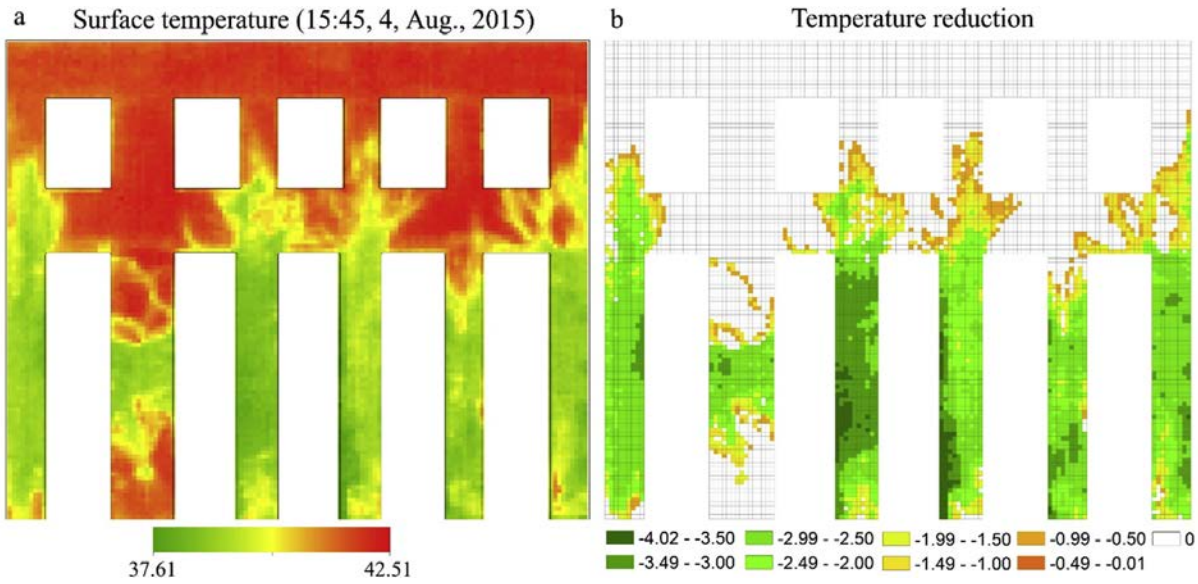

Fig. 3. Pixel-scale surface temperatures Ti and their reduction (DTi) for one scene.

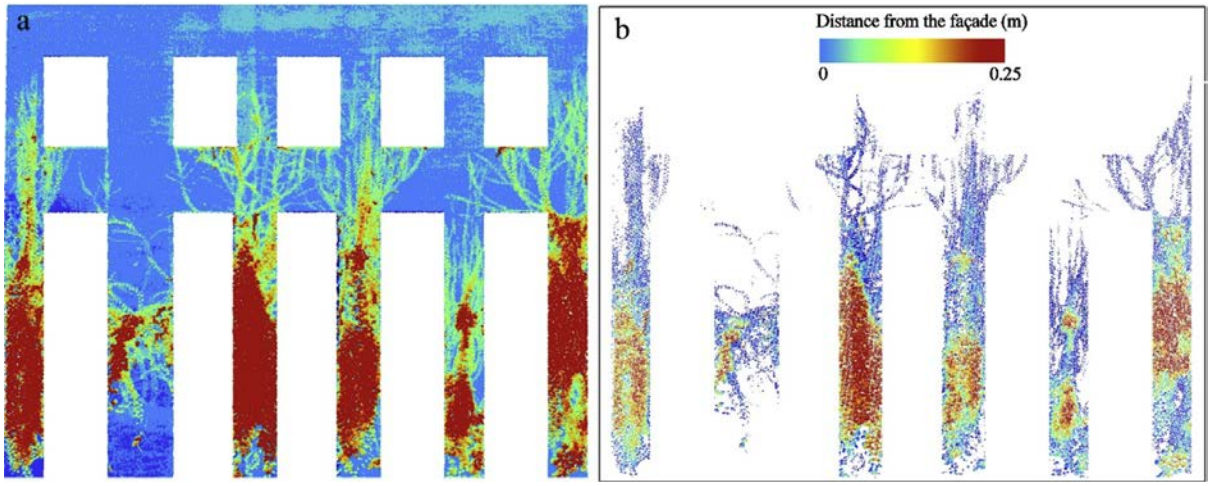

Fig. 4. 3DPC data for the building façade with windows excluded (a); selected points of the DGF vegetation (b).

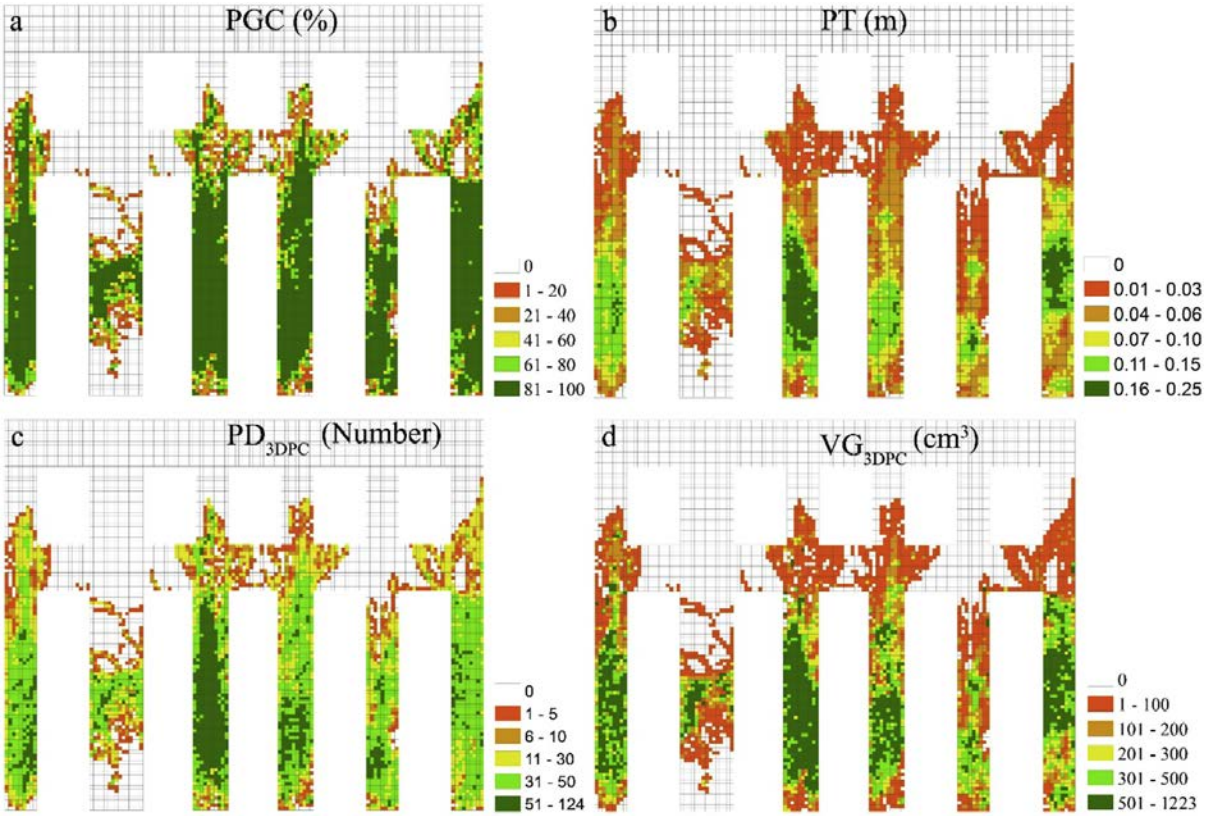

Fig. 5. Spatial distribution of the four plant parameters at the pixel scale: (a) Percentage of Green Coverage PGC); (b) Plant thicknesses (PT); (c) Point density PD3DPC; (d) Plant volume VG3DPC.

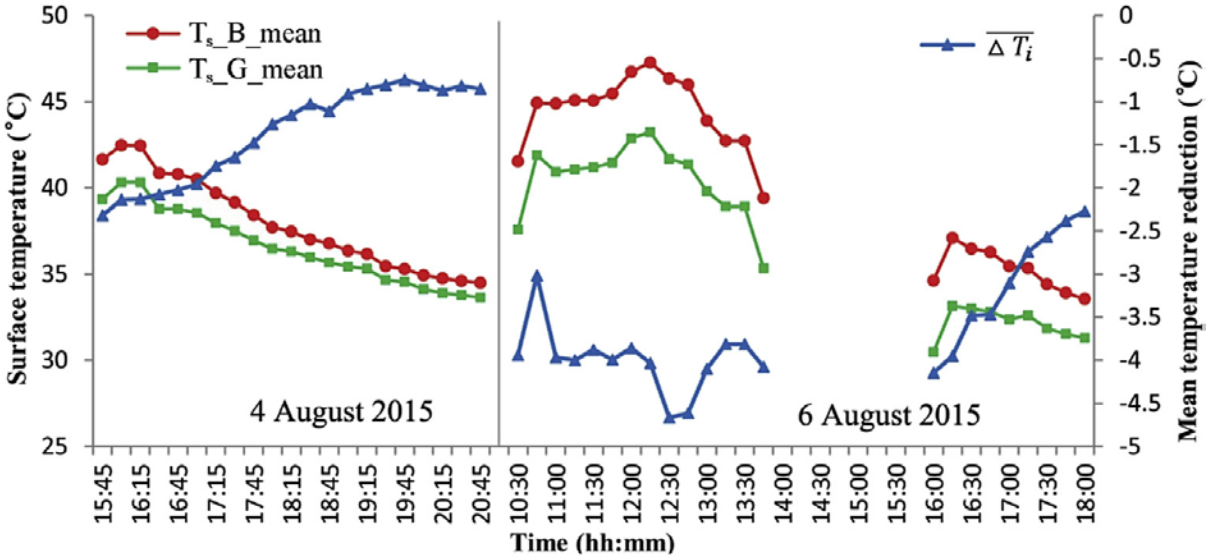

Fig. 6. Mean surface temperature and surface temperature reduction from the green façade for August 4 and August 6, 2015.

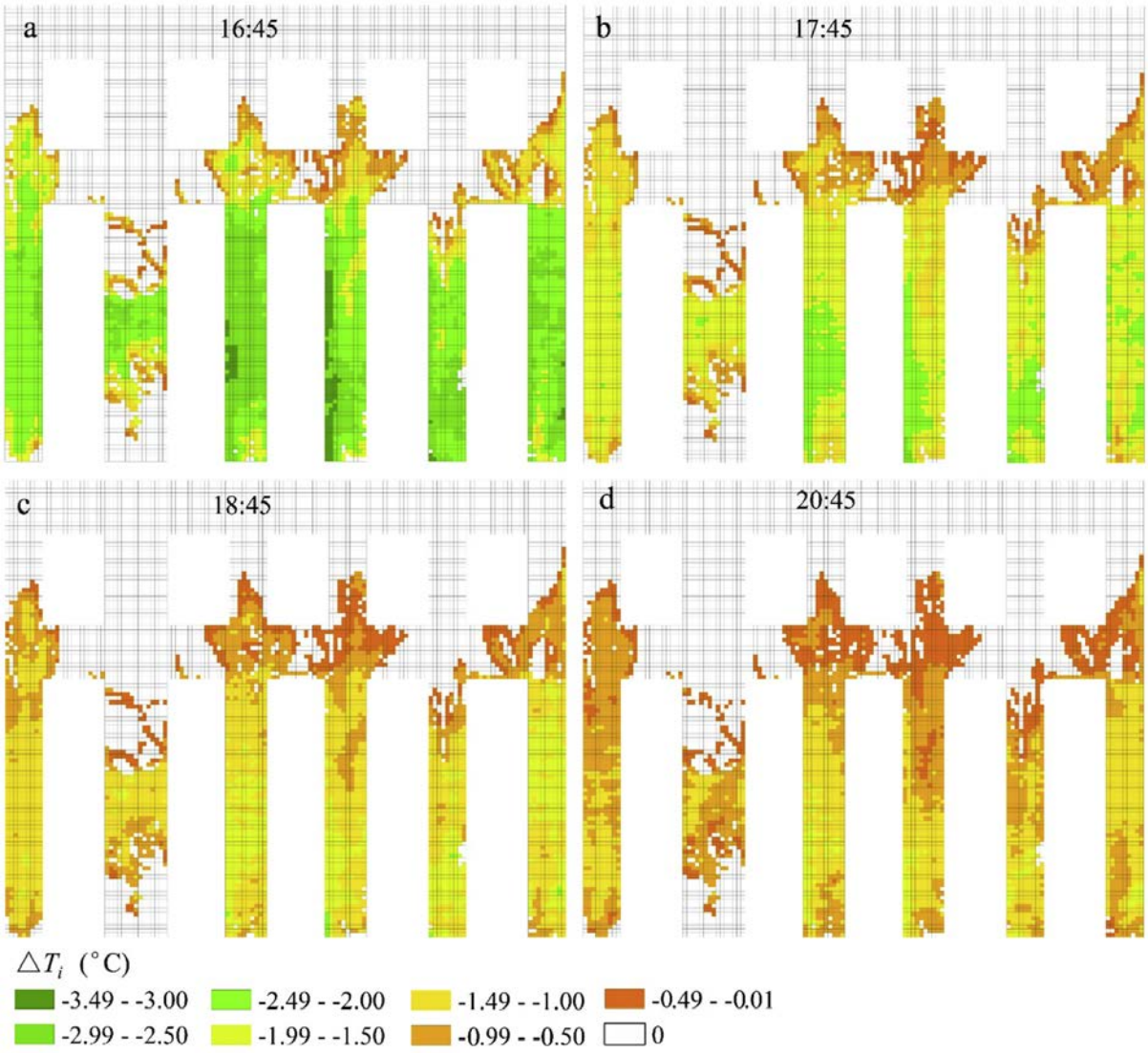

Fig. 8. Surface temperature reduction (DTi) at the pixel scale at selected times on August 4, 2015.

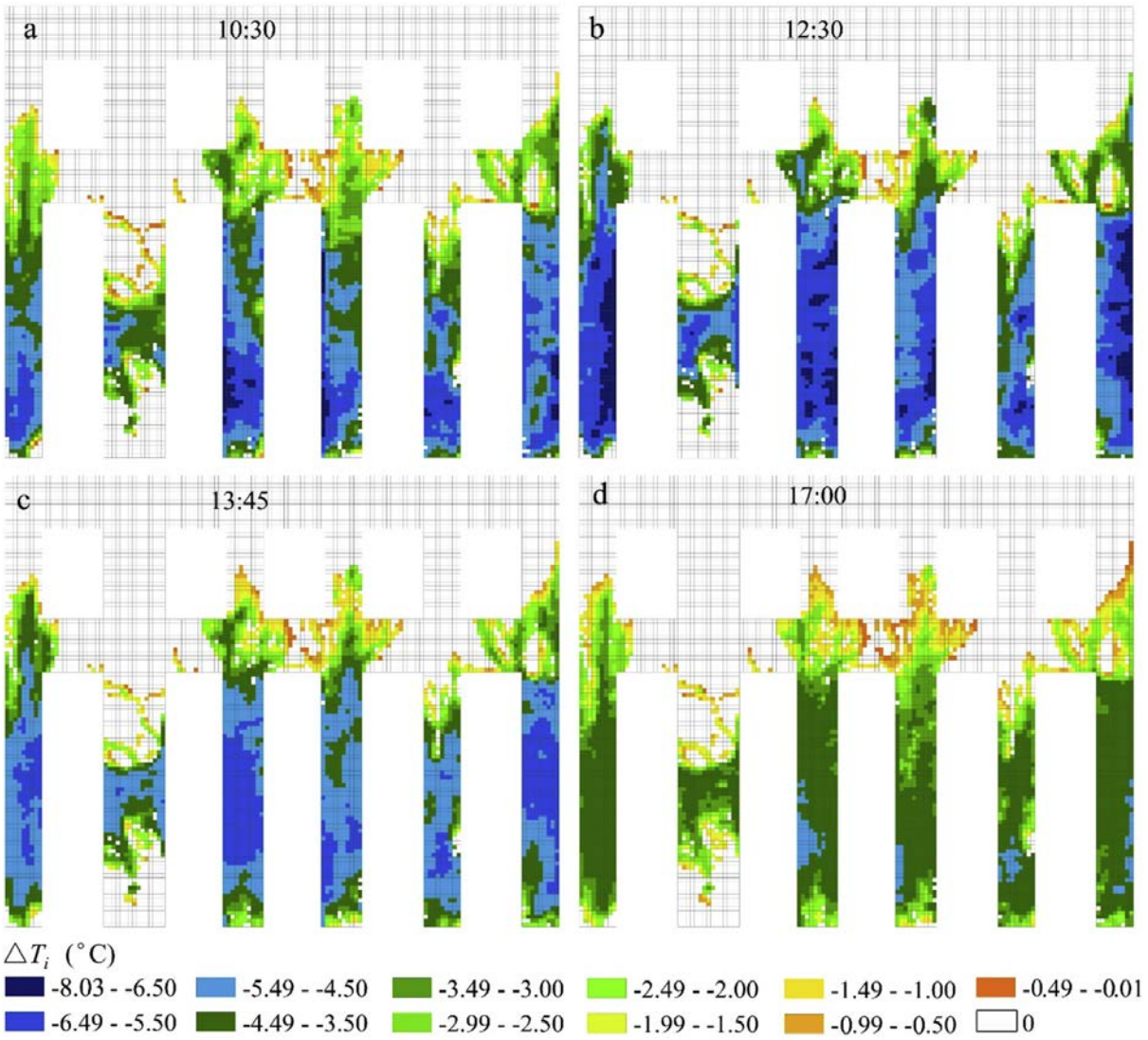

Fig. 9. Surface temperature reduction (DTi) at the pixel scale at selected times on August 6, 2015.

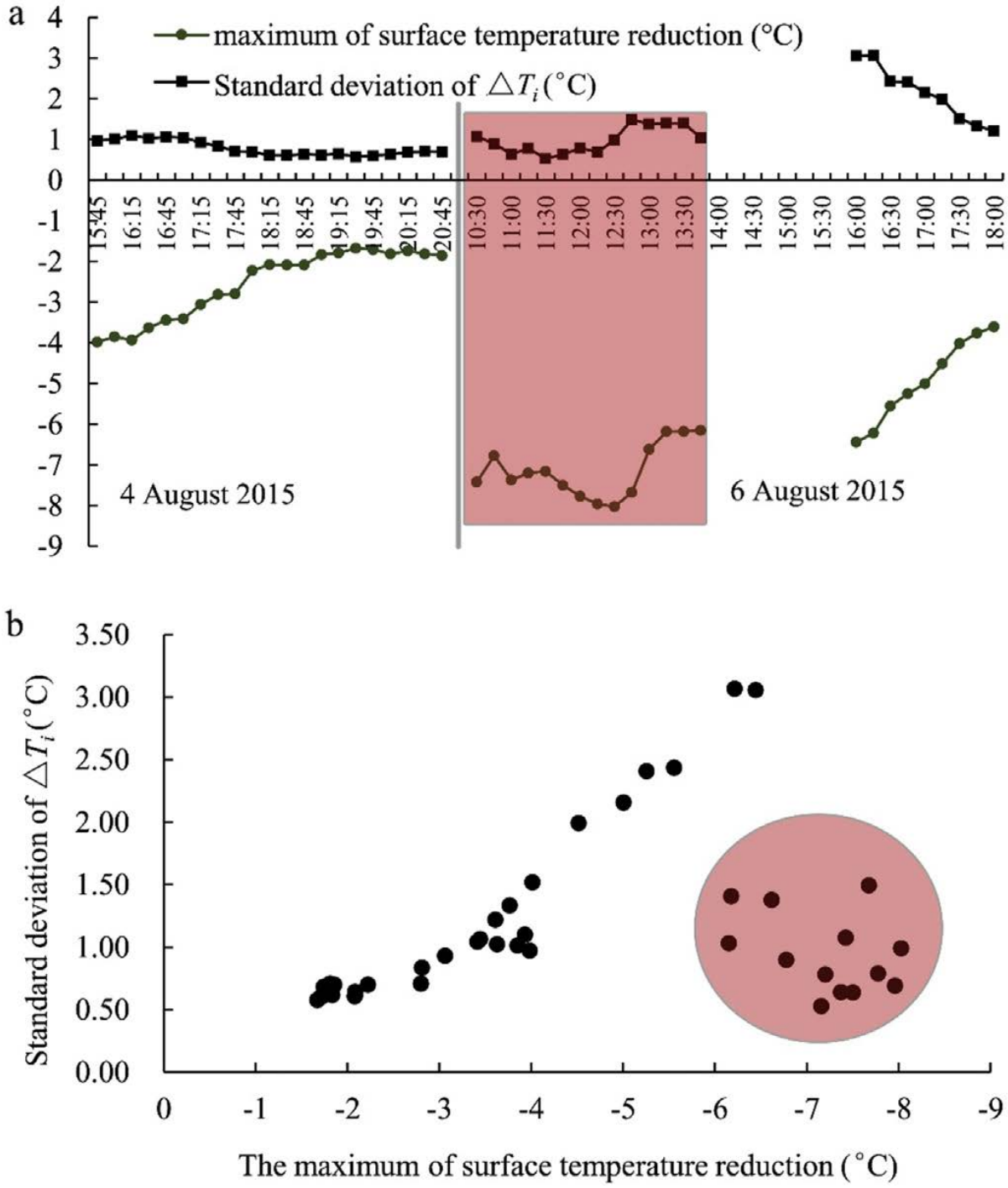

Fig. 10. Variation in the maximum DTi and the standard deviation of DTi.

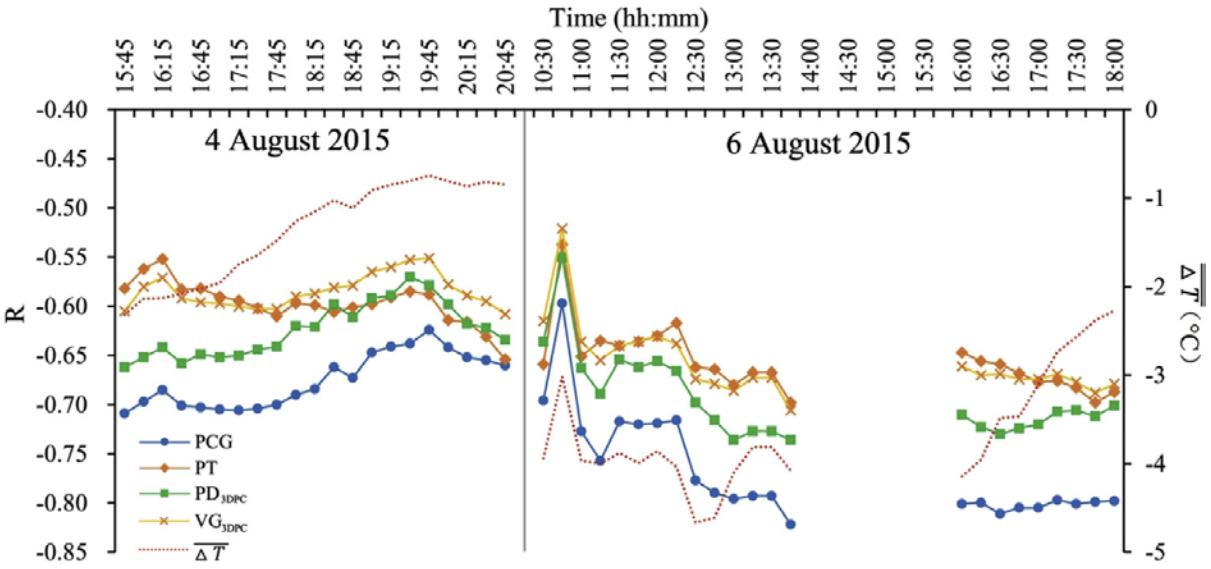

Fig. 11. Variation in the Pearson correlation coefficient between four plant characteristics and DT.

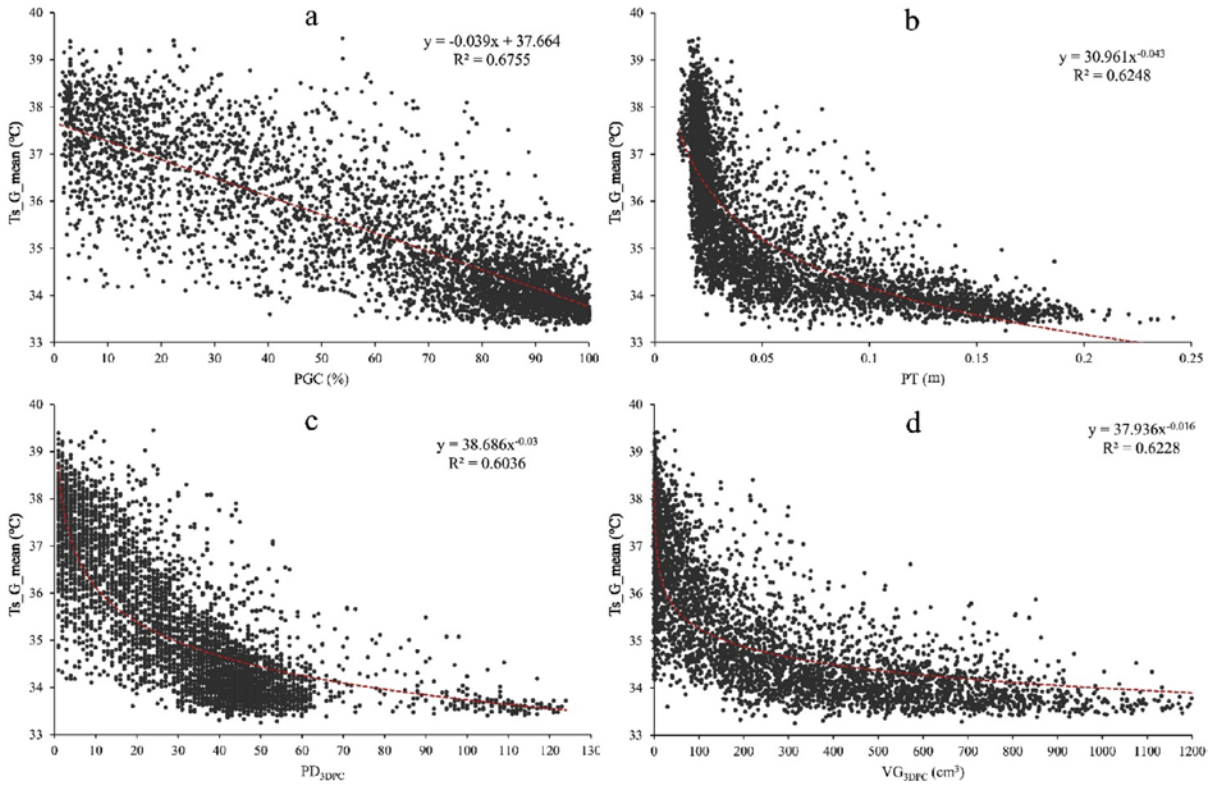

Fig. 12. Univariate regression relationships between four plant characteristics and Ts_G_mean at 13:45 h on August 6, 2015.